Annals of Clinical Microbiology and Antimicrobials

RESEARCH

Open Access

Proteomic analysis of carbapenem-resistant *Klebsiella pneumoniae* outer membrane vesicles under the action of phages combined with tigecycline

Jing Mao[1,2,4†], Xiaoyu Yang[2,3†], Cheng Yan[1,2,4], Fan Wang[1,2*] and Rui Zheng[1,2*]

Abstract

Background *Klebsiella pneumoniae* is the most commonly encountered pathogen in clinical practice. Widespread use of broad-spectrum antibiotics has led to the current global dissemination of carbapenem-resistant *K. pneumoniae*, which poses a significant threat to antibacterial treatment efficacy and public health. Outer membrane vesicles (OMVs) have been identified as carriers capable of facilitating the transfer of virulence and resistance genes. However, the role of OMVs in carbapenem-resistant *K. pneumoniae* under external pressures such as antibiotic and phage treatments remains unclear.

Methods To isolate and purify OMVs under the pressure of phages and tigecycline, we subjected *K. pneumoniae* 0692 harboring plasmid-mediated bla_{NDM-1} and bla_{KPC-2} genes to density gradient separation. The double-layer plate method was used to isolate MJ1, which efficiently lysed *K. pneumoniae* 0692 cells. Transmission electron microscopy (TEM) was used to characterize the isolated phages and extract OMV groups for relevant morphological identification. Determination of protein content of each OMV group was conducted through bicinchoninic acid assay (BCA) and proteomic analysis.

Results *K. pneumoniae* 0692 released OMVs in response to different environmental stimuli, which were characterized through TEM as having the typical structure and particle size of OMVs. Phage or tigecycline treatment alone resulted in a slight increase in the mean protein concentration of OMVs secreted by *K. pneumoniae* 0692 compared to that in the untreated group. However, when phage treatment was combined with tigecycline, there was a significant reduction in the average protein concentration of OMVs compared to tigecycline treatment alone. Proteomics showed that OMVs encapsulated numerous functional proteins and that under different external stresses of phages and tigecycline, the proteins carried by *K. pneumoniae* 0692-derived OMVs were significantly upregulated or downregulated compared with those in the untreated group.

†Jing Mao and Xiaoyu Yang contributed equally to this work.

*Correspondence:
Fan Wang
wfkunhua@126.com
Rui Zheng
ynkmzheng@gmail.com
Full list of author information is available at the end of the article

Conclusions This study confirmed the ability of OMVs to carry abundant proteins and highlighted the important role of OMV-associated proteins in bacterial responses to phages and tigecycline, representing an important advancement in microbial resistance research.

Keywords Carbapenem-resistant *Klebsiella pneumoniae*, Tigecycline, Phages, Outer membrane vesicles, Proteomics

Background

Klebsiella pneumoniae is a Gram-negative opportunistic pathogen that causes extremely serious infections with very high morbidity and mortality rates. Carbapenems are considered the last line of defense against drug-resistant Gram-negative bacterial infections in clinical practice. However, the latest monitoring data released by CHINET in August 2023 showed that the resistance rate of *K. pneumoniae* to carbapenems was expected to increase from 2.9 to 26.2% between 2005 and 2023 [1]. Therefore, carbapenem-resistant *K. pneumoniae* is recognized as one of the major pathogens causing hospital-acquired infections worldwide, posing a great challenge to hospital infection control measures [2].

As antimicrobial resistance (AMR) has become a growing public health threat, there is now a pressing need for alternative therapies, which has revitalized phage research [3]. As a type of viral particle prevalent in nature, phages can specifically infect host bacteria and are becoming a favorable treatment option for infections in clinical practice [4]. Phages infect their host bacteria by binding to their outer membrane or one of its components [5]. Outer membrane vesicles (OMVs) consist of the outer membrane of Gram-negative bacteria, which may play an important role in the interaction between bacteria and phages. Moreover, OMVs are spherical vesicles consisting of phospholipid (PL) bilayer membrane structures and membrane contents released externally by most Gram-negative bacteria [6, 7]. Ranging in diameter from 20 to 200 nm, OMVs may contain PLs, outer membrane proteins, lipopolysaccharide, DNA, RNA, bacterial metabolites, and signaling molecules, among other components [8, 9]. As part of the secretory delivery system, OMVs allow the dissemination of bacterial components into the environment, facilitating cell-to-cell interactions without the need for direct contact [10]. Therefore, OMVs play a key role in the response to environmental pressures such as phages and antibiotics.

Earlier work by Loeb showed that in the presence of a T4 phage in *Escherichia coli*, the production and release of OMVs were significantly increased [11]. Furthermore, the production of OMVs when phages are adsorbed onto bacterial surfaces has also been linked to bacterial defense and protection mechanisms [12]. Notably, antibiotics combined with phages for multidrug-resistant *Pseudomonas aeruginosa* exhibit synergistic activity. Despite the presence of acquired resistance mechanisms in bacteria, including overexpression of efflux pumps and expression of protein channels, phages can reduce the production of OMVs, which may contribute to the reduction of resistance and increase the efficacy of antibiotics [13].

Detecting and analyzing the expression types and levels of bacterial OMV-associated proteins will be useful for determining the optimal phage-antibiotic combinations for organisms with specific acquired resistance mechanisms and identifying the key mechanisms behind the relationship between phage-combined antibiotics and OMVs. In this study, we focused on a clinically isolated carbapenem-resistant *K. pneumoniae* strain that was resistant to all antibiotics tested, except tigecycline, to elucidate the protein composition and biological functions of OMVs under pressure from drugs and phages. These findings may contribute to the prevention and control of carbapenem-resistant *K. pneumoniae* infections, help in understanding the pathogenic mechanisms involved, and promote the development of OMVs.

Methods

Bacterial strains

The *K. pneumoniae* 0692 strain used in this study, harboring two carbapenemases, NDM-1 and KPC-2, was isolated from the First People's Hospital of Yunnan Province, China. It was identified simultaneously using the VITEK 2 Compact and VITEK MS systems (bioMérieux, Lyon, France).

Bacterial drug-resistant gene detection

Plasmid DNA was extracted using a plasmid extraction kit (Tiangen, Beijing, China). The bla_{NDM} and bla_{KPC} plasmids were identified using polymerase chain reaction (PCR) and sequencing.

DNA extraction and PCR

The extraction of genomic DNA from *K. pneumoniae* 0692 isolates was performed with a bacterial genomic DNA extraction kit (Tiangen, Beijing, China). Table 1 lists the specific primers. Set up the PCR reaction system and amplification programme according to the Master Mix instructions (TSINGKE, China).

Table 1 List of primers used in this study

Primer	Sequence (5′ to 3′)
NDM-Forw	GGTTTGGCGATCTGGTTTTC
NDM-Rev	CGGAATGGCTCATCACGATC
KPC-Forw	CGTCTAGTTCTGCTGTCTTG
KPC-Rev	CTTGTCATCCTTGTTAGGCG

Whole-genome sequencing of *K. pneumoniae* 0692 and phages

The genomic DNA of the clinically isolated *K. pneumoniae* 0692 strain was extracted using the Bacterial Genomic DNA Extraction Kit (Tiangen, China) and sequenced using the PacBio Sequel II/PacBio Sequel IIe and Illumina NovaSeq PE150 sequencing platforms. Similarly, phage genomic DNA was extracted using the Phage λ Genomic DNA Extraction Kit (Yuanye Biology, China) and sequenced using Illumina NovaSeq sequencing platforms following the manufacturer's instructions. The sequencing results were compared with NCBI blast (https://blast.ncbi.nlm.nih.gov/Blast.cgi).

Determination of the minimum inhibitory concentrations (MICs)

The MICs of antimicrobial agents were determined using the microdilution susceptibility testing method. The following antibiotics were tested: imipenem, meropenem, ertapenem, tigecycline, ceftazidime/avibactam, cefoxitin, amikacin, and aztreonam. MIC results were interpreted as specified by Clinical Laboratory Standards Institute (CLSI) guidelines [14], except for tigecycline, which followed the interpretation defined by the US Food and Drug Administration (susceptible: MIC ≤ 2 mg/L; resistant: MIC ≥ 8 mg/L). *Escherichia coli* ATCC 25922 and *Pseudomonas aeruginosa* ATCC 27853 were used as quality controls.

Isolation and purification of phages

Phage isolation and purification were performed using the double-layer plate method, as previously described [15]. In brief, 100 µL of *K. pneumoniae* 0692 microbial suspension from an overnight culture and 100 µL of untreated sewage filtered through a 0.22 µm membrane filter (Thermo Fisher Scientific, USA) were mixed with 10 mL of fresh LB medium (Coolaber, China). The mixture was incubated in a shaking incubator at 160 rpm and 37 °C, and the resulting culture solution was filtered through a 0.22 µm filter to retain the filtrate. The lower plate of LB solid medium (2% agar) was prepared, and the upper plate was prepared by mixing 100 µL of overnight cultured *K. pneumoniae* 0692 and 100 µL of culture filtrate in semi-solid LB medium (0.5% agar), then spreading the plate and incubating at 37 °C overnight. Transparent round phage spots on top of the background of the host bacterium were observed. Single phage spots were picked and mixed into the *K. pneumoniae* 0692 microbial suspension to prepare double-layer plates for further purification. At least three rounds of purification were performed to efficiently lyse *K. pneumoniae* 0692. Plates with 30–300 phage spots were selected for counting. Titer (potency) = (number of phage spots × dilution × 10) PFU/mL.

Isolation and purification of OMVs

OMVs were prepared through density gradient ultracentrifugation in the absence or presence of 2 µg/mL tigecycline (MedChemExpress, Monmouth Junction, NJ, USA) and phage, following previously established protocols with minor adjustments [16]. Briefly, single colonies grown on LB agar plates were inoculated into 20 mL of LB broth medium (OD600 = 0.4). Subsequently, 1 mL of the microbial suspension was inoculated into 300 mL of antibiotic (2 µg/mL tigecycline) or phage-containing (1 mL of phage [1.42×10^{10} PFU/mL] solution added to 300 mL of LB medium) solutions and then incubated at 37 °C with shaking at 150 rpm for 16 h. Cultures were taken at 8000 rpm for 30 min at 4 °C to remove bacteria and cellular debris. The supernatant after centrifugation was collected and filtered using a 0.22 µm filter to remove fine debris. After the supernatant was ultracentrifuged at 25,000 rpm for 50 min at 4 °C in a P100AT2 rotor (Hitachi CP-100WX, Japan), the pellet was resuspended in 8 mL of phosphate-buffered saline (PBS) (Servicebio, China). OptiPrep™ (Sigma-Aldrich, Germany) was used to prepare 10%, 20%, and 30% density gradient solutions, which were distributed into discrete 10–30% density gradient layers. The resuspended OMV samples were placed on the density gradient and centrifuged at 4 °C and 25,000 rpm for 2 h. The OMV layer was collected and purified by washing with a tenfold volume of PBS solution at 25,000 rpm and 4 °C for 30 min. The resulting pellet was resuspended with 5 mL of PBS to obtain purified OMVs. The purified OMV solution was passed through a 0.22 µm membrane filter and filtered again. External DNA and proteins were removed using 2U DNase I (Biosharp, China) and 100 µg/mL Protease K (Biosharp, China). Purified OMV solution was inoculated onto Columbia blood plates to verify sterility.

Transmission electron microscopy

Purified phages and OMVs were observed through transmission electron microscopy (TEM). Samples were prepared by applying 10 µL of phage or OMVs suspended in PBS onto a carbon-coated copper grid for 5 min. After drying, the samples were stained with 2% uranyl acetate

(Bio-Rad, Hercules, CA, USA) for 2 min, and the excess liquid was blotted. Observations were performed using a JEM-1400 Plus TEM (JEOL, Tokyo, Japan), operating at 80 kV.

Protein quantification of OMVs

Approximately 50 µL of OMVs were treated with 2U of DNase I (Biosharp, China) and 100 µg/mL of Protease K (Biosharp, China), followed by the addition of 50 µL of RIPA lysate (Beyotime, China). The mixture was then incubated at 4 °C for 30 min and subsequently centrifuges at 10,000×*g* at 4 °C for 15 min. A bicinchoninic acid (BCA) protein assay kit (Biosharp, China) was used to determine the protein concentration of OMVs samples, according to the manufacturer's protocols.

Mass spectrometry assay of OMVs

The mass spectrometry experimental analysis process involved protein extraction, peptide enzymolysis, liquid chromatography-tandem mass spectrometry, and database retrieval. Briefly, SDT buffer (4% SDS, 100 mM Tris–HCl, pH 7.6; Bio-Rad, USA) was directly added to the different samples. DTT (with a final concentration of 40 mM; Bio-Rad, USA) was added to each sample individually and mixed at 600 rpm for 1.5 h (37 °C). After the samples were cooled to room temperature, iodoacetamide (Bio-Rad, USA) was added at a final concentration of 20 mM to block the reduced cysteine residues. Subsequently, the samples were incubated for 30 min in the dark, then transferred to filters (MicroCon units, 10 kDa). The filters were washed thrice with 100 µL UA buffer, then twice with 100 µL 25 mM NH_4HCO_3 (Sigma, Germany) buffer. Finally, trypsin was added to the samples (at a trypsin: protein (wt/wt) ratio of 1:50; Promega, Madison, WI, USA) and incubated at 37 °C for 15–18 h (overnight). The resulting peptides were collected as the filtrate. The peptides from each sample were analyzed using an Orbitrap™ Astral™ mass spectrometer (Thermo Scientific, USA) connected to a Vanquish Neo system liquid chromatograph (Thermo Scientific, USA) in data-independent acquisition (DIA) mode. DIA data were analyzed using DIA-NN 1.8.1 software.

Results

Bacterial drug-resistant gene detection

As demonstrated in Fig. 1 (Supplementary Material 2), DNA purified from the *K. pneumoniae* 0692 isolate exhibited specific amplified products for *KPC* and *NDM* (The lengths of the PCR products were *KPC*-752 bp and *NDM*-595 bp, Supplementary Material 1). Moreover, Whole-genome sequencing results were compared with NCBI blast (https://blast.ncbi.nlm.nih.gov/Blast.cgi) showed that *K. pneumoniae* 0692 harbored both $bla_{\text{NDM-1}}$ and $bla_{\text{KPC-2}}$.

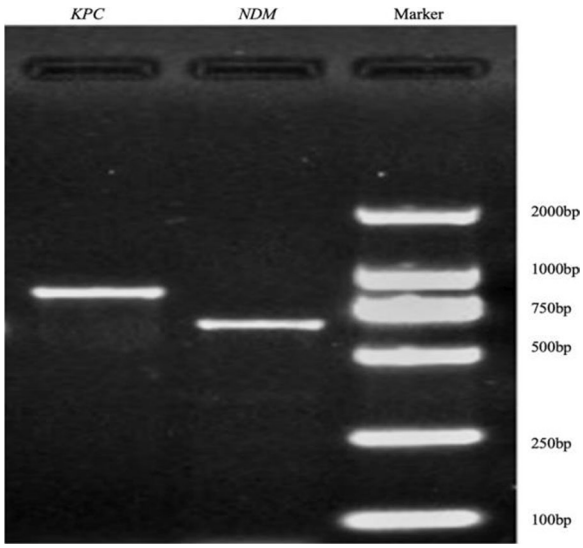

Fig. 1 PCR profile of the strain used in this study. The primers used to perform PCR are *KPC* (left), *NDM* (middle) and the marker DL2000 (right), respectively

Table 2 Results of MIC determination

Antibiotic	MIC (µg/mL)	Sensitivity results
Imipenem	128	R
Meropenem	> 128	R
Ertapenem	> 128	R
Tigecycline	1	S
Ceftazidime/avibactam	> 128/4	R
Cefoxitin	> 128	R
Amikacin	> 128	R
Aztreonam	> 64	R

R resistant, *I* intermediary, *S* susceptible

Antimicrobial susceptibility testing

K. pneumoniae 0692 was resistant to cephalosporins, carbapenems, aminoglycosides, and β-lactams/β-lactamase inhibitors. However, this strain was sensitive to tigecycline with a MIC of 1 µg/mL. The results of the drug sensitivity tests are presented in Table 2. Based on the drug sensitivity results, tigecycline was administered to induce OMVs production.

Isolation and biological characterization of phages

K. pneumoniae 0692 phages, named MJ1, were isolated from the sewage of the First People's Hospital of Yunnan Province, using *K. pneumoniae* 0692 as the host. The phage plaque formed by MJ1 had a transparent

appearance and a diameter of 3–4 mm. The phage concentration was determined to be approximately 1.42×10^{10} PFU/mL by titer (Fig. 2A, B). Morphologically, MJ1 displayed a polyhedral stereosymmetric head with a diameter of approximately 100 nm and a long tail, as observed through TEM. The genome length of phage MJ1 measured 111,163 bp in length, with a G+C% content of 44.72%, and comprised 1,385 open reading frames. According to the virus classification standards outlined by the International Committee on Taxonomy of Viruses in 2022, MJ1 phages are classified within the *Myoviridae* family.

Detection of OMVs

K. pneumoniae 0692 was cultured with or without 2 μg/mL tigecycline as well as phages, and purified OMVs were extracted from *K. pneumoniae* 0692 cultured under different conditions using density gradient centrifugation (Fig. 3A–D). TEM showed confirmed the spherical nature of the purified OMVs. No bacteria were detected under a light microscope, and cultures of the OMVs on Columbia blood culture plates showed no bacterial growth, indicating successful purification (Fig. 3). The mean particle size and protein concentration of each OMV group is shown in Table 3. The protein concentration in OMVs increased 1.33-, 4.38-, and 3.03-fold when *K. pneumoniae* 0692 was treated with phages, tigecycline, and phages with tigecycline, respectively. The average diameter of OMVs decreased after treatment with tigecycline, regardless of whether it was combined with phages.

The results are summarized in Table 3. The mean particle size of each OMV group was analyzed through TEM, and the mean protein concentration of the OMVs was determined using a BCA protein assay kit (Biosharp, China).

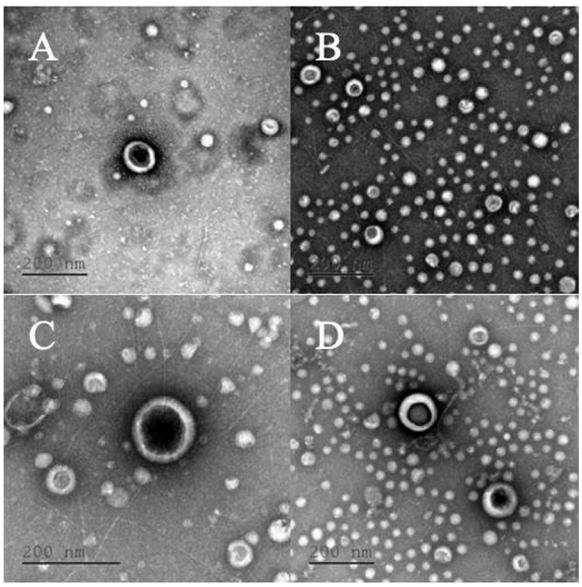

Fig. 3 **A** OMVs extracted without treatment (M). **B** OMVs extracted following treatment with 2 μg/mL tigecycline (MT). **C** OMVs extracted following phage treatment (MP). **D** OMVs extracted following co-treatment with 2 μg/mL tigecycline and phage (MTP). Scale bar: 200 nm

Proteomic analysis of different OMVs

Proteins from OMVs were digested on a gel with trypsin and extracted from the gel for proteomic analysis. Differential protein expression in OMVs from group M was compared with that of other groups separately. The proteomic analysis revealed a significant decrease in the gpmA protein across all groups. Formate-dependent phosphoribosylglycinamide formyltransferase (purT) protein expression was significantly upregulated in the MT group, whereas the 60 kDa chaperonin (groEL) protein was significantly upregulated in the MP group compared to that in the untreated group. Simultaneous treatment with tigecycline and phages resulted in significant upregulation of purT, groEL and thioredoxin (trxA)

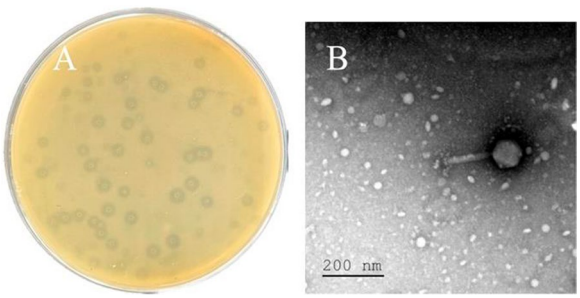

Fig. 2 **A** Isolation and purification via the bilayer plate method to obtain phage spots of lysed *K. pneumoniae* 0692. **B** Transmission electron observation of phage morphology. Scale bar: 200 nm

Table 3 The mean particle size and protein concentration of OMVs

Groups	Z-Average (nm)	Average protein concentration (μg/μL)
M	90.46	0.86
MT	51.29	3.77
MP	95.39	1.14
MTP	66.53	2.61

M OMVs extracted without treatment, *MT* OMVs extracted following treatment with 2 μg/mL tigecycline, *MP* OMVs extracted following phage treatment, *MTP* OMVs extracted following co-treatment with 2 μg/mL tigecycline and phage

proteins (Fig. 4). The subcellular localization of the differentially expressed proteins in OMVs detected in this study was determined using an online subcellular structure prediction website (http://www.csbio.sjtu.edu.cn/bioinf/Cell-PLoc-2/) [17], as shown in Table 4. Among the identified proteins, the most significantly enriched differentially expressed proteins were associated with cellular metabolic processes, biosynthesis, intracellular structures, and nucleic acid binding.

Table 4 Subcellular localization of differential proteins detected in this study

Genes	Protein descriptions	Subcellular localization
groEL; grosL	Chaperonin GroEL 60 kDa chaperonin	Cytoplasm
gpmA	2,3-bisphosphoglycerate-dependent phosphoglycerate mutase	Cell inner membrane Cytoplasm
purT	Formate-dependent phosphoribosylglycinamide formyltransferase	Cell inner membrane Cytoplasm
trxA	Thioredoxin	Cytoplasm

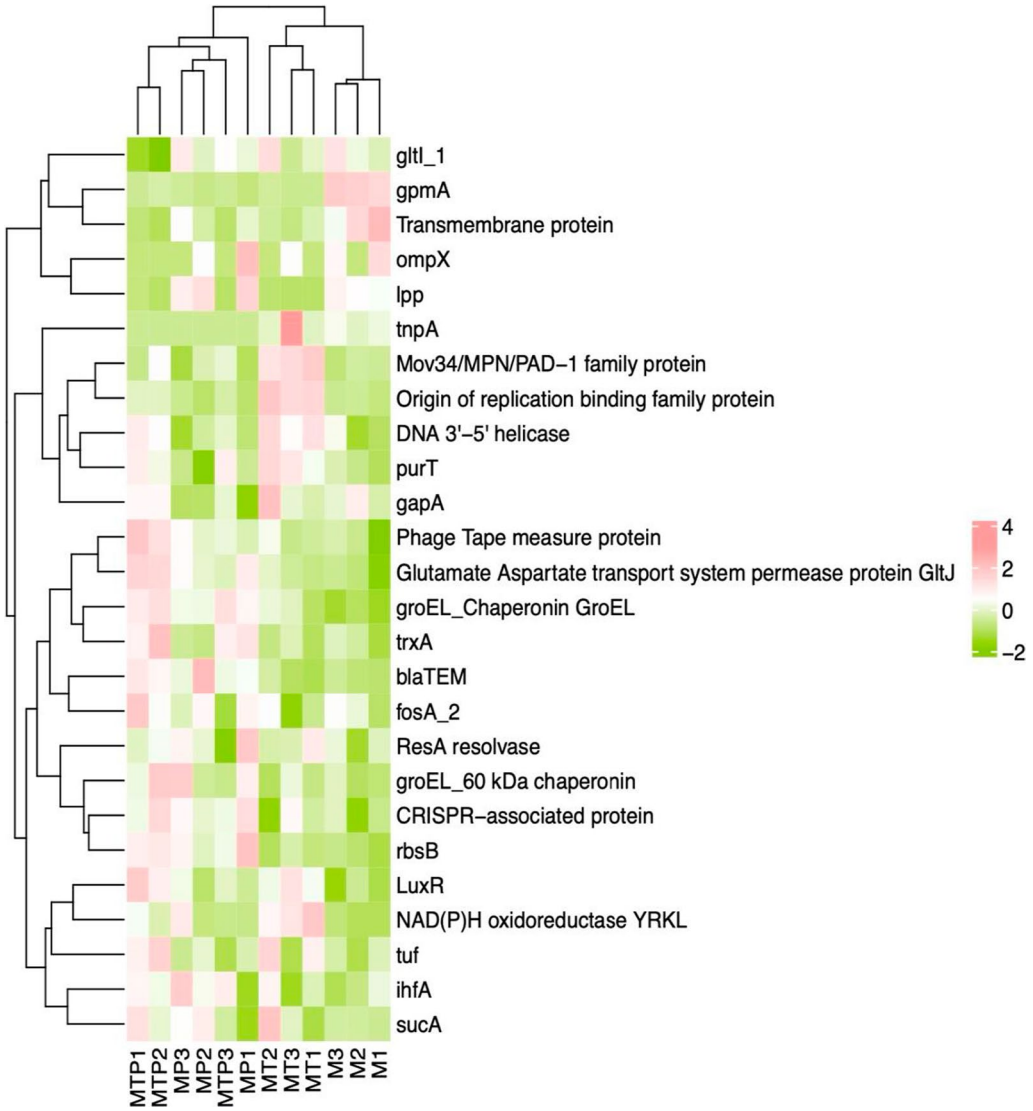

Fig. 4 Heatmap of significantly differentially expressed proteins. The results of hierarchical clustering were represented as a tree heat map. The horizontal axis represents the samples with different colors to indicate sample grouping information. The vertical axis represents differentially expressed proteins, with significant changes denoted by vertical coordinates. Significantly differentially expressed proteins across samples were normalized using the Z-score method and are presented in the heatmap with no colors. The red color indicates significantly upregulated proteins, the green color represents significantly downregulated proteins, and the grey color represents no protein quantification information

Discussion

Carbapenem-resistant *K. pneumoniae* stands as a prominent clinical pathogen, with NDM-1 and KPC-2 being the prevailing carbapenems posing significant threats to global public health [18]. Exploring the mechanisms of drug resistance in carbapenem-resistant *K. pneumoniae* and new combinations of therapies is conducive to further improving outcomes and developing cures for infections caused by carbapenem-resistant *K. pneumoniae*.

In this study, we isolated OMVs from *K. pneumoniae* 0692 alone and with the addition of phages and tigecycline. TEM examination revealed morphological differences in OMVs, particularly in particle size (Fig. 3). Notably, treatment with tigecycline led to a reduction in the average particle size of OMVs. We hypothesized that the smaller OMVs secreted in response to tigecycline treatment could potentially alter the outer membrane structure, thereby inducing partial defects in OMVs synthesis.

In the presence of phages, tigecycline, and phages with tigecycline, the protein concentration in OMVs increased by 1.33-, 4.38-, and 3.03-fold. To elucidate the changes in the proteins in OMVs, proteomic analyses of different groups of OMVs were performed. We observed significant differences in the protein expression in OMVs after induction with tigecycline, phages, or both. Four differentially expressed proteins were identified: gpmA, purT, groEL, and trxA (Table 4). These proteins are associated with energy metabolism processes, catalytic activities, and chaperone functions, suggesting their potential importance in phages and drugs (Fig. 5).

In the MT, MP, and MTP groups, we observed a significant down-regulation of the 2, 3-bisphosphoglycerate-dependent phosphoglycerate mutase protein after tigecycline and phage treatment. This enzyme, encoded by *gpmA*, is known to be involved in glycolysis and plays a crucial role in bacterial energy metabolism [19]. In addition, *gpmA* functions as a member of the bacterial oxidative stress defense mechanism and influences bacterial tolerance to the external environment [20]. Previous studies have isolated actinomycin D, a potent natural anti-methicillin-resistant *Staphylococcus aureus* (anti-MRSA) agent, from *Streptomyces maritimus*. Actinomycin D has demonstrated potential anti-MRSA activity by downregulating the mRNA expression level of the key differential protein gpmA, thereby inducing a novel metabolic pathway that promotes antibiotic susceptibility in MRSA [21]. Because this protein is associated with biofilm formation and antibiotic susceptibility, we hypothesized that tigecycline in combination with phages may exert antibacterial effects by influencing bacterial energy metabolism and biofilm formation.

When treated with tigecycline alone (MT group), the significantly differentially expressed protein was found to be formate-dependent purT, which showed significant upregulation in its expression after tigecycline induction compared with that in the untreated group. Notably, purT from *E. coli* encodes a glycine amide ribonuclease (or purT-converting enzyme) that belongs to the ATP-grasp superfamily and requires the co-catalysis of Mg^{2+} ATP and formate to promote the formylation of glycine amide ribonucleotides for purine biosynthesis [22, 23]. Furthermore, cytoHubba analysis based on transcriptomic profiles demonstrated that *purT* is the hub gene for resistance to fluoroquinolones, and that the upregulation of *purT* affects bacterial resistance to antibiotics [24]. In this study, we hypothesized that in response to the effects of tigecycline, the *K. pneumoniae* 0692 strain releases purT enzymes to improve its survival.

In the MP group, we observed that GroEL was significantly upregulated in OMVs. This increase suggests that tigecycline or phage treatment enhances the bacteria's ability to prevent protein misfolding under stressful conditions [25]. Previous studies have proposed that aminoglycosides cause cytosolic protein misfolding, and that chaperonin GroEL/GroES overexpression counters this defect, leading to aminoglycoside resistance [26, 27]. In our study, an increase in GroEL expression was also observed with phage treatment, suggesting that the phage is ineffective when combined with aminoglycosides. Therefore, exploring an optimal therapeutic regimen for phages and antibiotics is essential for addressing bacterial drug resistance.

Furthermore, in the MTP group where tigecycline and phages were administered concurrently, we observed differential expression of not only gpmA and purT proteins but also a third protein, TrxA. The TrxA system is an important contributor to cellular redox balance, regulates cell growth, apoptosis, gene expression, and antioxidant defense in nearly all living cells, and is one of the key regulators of the proliferative potential of cells through the reduction of key proteins [28]. Increased oxidative stress is characterized by highly proliferative, metabolically hyperactive cells, which are forced to mobilize antioxidant enzymes to balance the increase in free radical concentration and prevent irreversible damage and cell death. However, the role of TrxA in antibiotic drug resistance remains unclear [29]. We speculate that TrxA protects organisms from antibiotic and phage attacks by playing a role in redox signaling and acting as a redox-independent cellular chaperone [30]. Bacteriophage T7 can use the TrxA of its host, *E. coli*, to enhance the processivity of its DNA polymerase, thus increasing the ability of the phage to act on host bacteria [31]. TrxA reductase encapsulated in OMVs was significantly

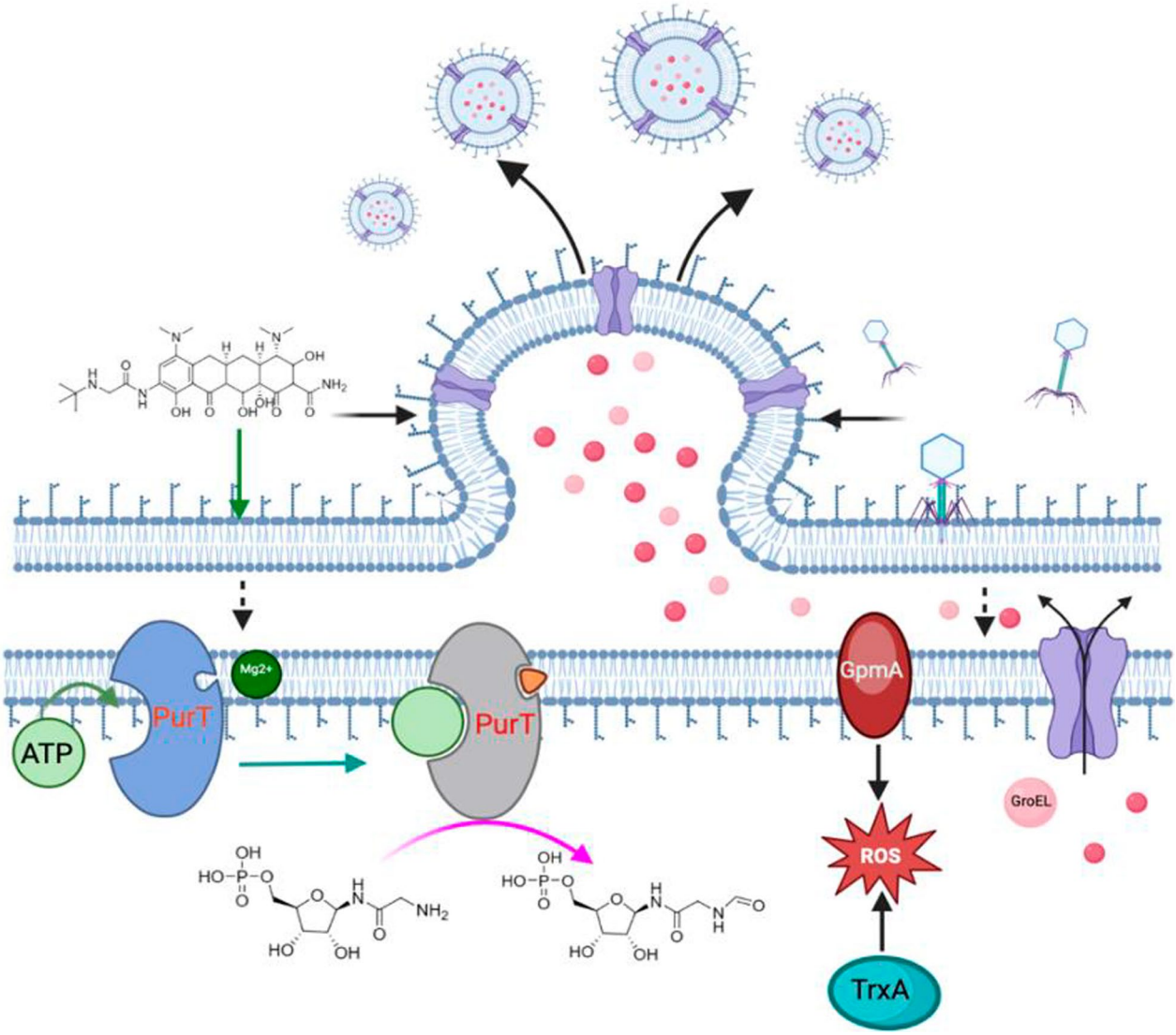

Fig. 5 Schematic diagram depicting significantly altered OMV proteins gpmA, purT, groEL, and trxA, which are involved in are prosess to environment pressure. The figure was designed using Biorender

upregulated in the presence of tigecycline and phage compared with that in the untreated group, suggesting that this protein plays an important role in response to the action of external environmental pressure. Further studies into its mechanism of action will enhance our understanding of tigecycline and phage antibacterial mechanisms.

In summary, carbapenem-resistant *K. pneumoniae* demonstrated the ability to produce and release OMVs under the influence of tigecycline and phages, encapsulating numerous proteins vital for bacterial survival and energy metabolism. These differentially expressed proteins warrant further exploration to decipher the interaction mechanisms among phages, antimicrobial drugs, and bacterial vesicles, offering potential solutions to the pressing issue of AMR.

Conclusions

Our study demonstrated that under external environmental pressures, such as exposure to tigecycline or phages, OMVs derived from *K. pneumoniae* 0692 can disrupt the cell membrane by encapsulating relevant cell membrane proteins, thereby achieving a synergistic bactericidal effect. We have demonstrated that OMVs play an important role in synergizing the antibacterial effects of tigecycline and can enhance antibiotic effects by transporting protein cargoes while resisting external environmental pressures. Our research highlights the

important role of OMVs as "protein vectors" in bacterial responses to environmental changes.

Abbreviations

K. pneumoniae	*Klebsiella pneumoniae*
AMR	Antimicrobial resistance
OMVs	Outer membrane vesicles
MIC	Minimum inhibitory concentrations
CLSI	Clinical & Laboratory Standards Institute
BCA	Bicinchoninic acid assay
PBS	Phosphate-buffered saline
OD	Optical density
TEM	Transmission electron microscopy
DIA	Data-independent acquisition

Supplementary Information

The online version contains supplementary material available at https://doi.org/10.1186/s12941-024-00734-y.

Supplementary Material 1.

Supplementary Material 2.

Acknowledgements
We would like to thank the Institutional Center for Shared Technologies and Facilities of Kunming Institute of Zoology, Chinese Academy of Sciences for providing us with Transmission Electron Microscopy and Ultracentrifuge. We are grateful to Yingqi Guo for her great help in making TEM samples and taking/analyzing TEM images.

Author contributions
RZ and FW designed the study. RZ revised the manuscript. JM drafted the first version of this manuscript. XY analyze the data of Proteomic. JM and CY carried out the experiments. All authors read and approved the final manuscript.

Funding
This work was supported by the National Natural Science Foundation of China (grant No: 82160403), the Young and Middle-aged Academic and Technical Leaders Talent Project (Grant No. 202305AC160023), the Yunnan Science and Technology Commission (grant No: 202101AY070001-247) of the Yunnan Provincial Science and Technology Department and Kunming Medical University.

Availability of data and materials
No datasets were generated or analysed during the current study.

Declarations

Ethics approval and consent to participate
Not applicable.

Consent for publication
Not applicable.

Competing interests
The authors declare no competing interests.

Author details
[1]Department of Clinical Laboratory, The First People's Hospital of Yunnan Province, Kunming, Yunnan, China. [2]The Affiliated Hospital of Kunming University of Science and Technology, Kunming, Yunnan, China. [3]Regenerative Medicine Research Center, The First People's Hospital of Yunnan Province, Kunming, Yunnan, China. [4]The Affiliated Hospital of College of Medical, Kunming University of Science and Technology, Kunming, Yunnan, China.

Received: 30 April 2024 Accepted: 6 August 2024
Published online: 20 August 2024

References

1. CHINET. http://www.chinets.com; 2023.
2. Gomez-Simmonds A, Uhlemann AC. Clinical implications of genomic adaptation and evolution of carbapenem-resistant *Klebsiella pneumoniae*. J Infect Dis. 2017;215:S18-s27.
3. Knezevic P, Hoyle NS, Matsuzaki S, Gorski A. Editorial: advances in phage therapy: present challenges and future perspectives. Front Microbiol. 2021;12: 701898.
4. Khalid A, Lin RCY, Iredell JR. A phage therapy guide for clinicians and basic scientists: background and highlighting applications for developing countries. Front Microbiol. 2020;11: 599906.
5. Stern A, Sorek R. The phage-host arms race: shaping the evolution of microbes. BioEssays. 2011;33(1):43–51.
6. Kim JY, Suh JW, Kang JS, Kim SB, Yoon YK, Sohn JW. Gram-negative bacteria's outer membrane vesicles. Infect Chemother. 2023;55(1):1–9.
7. Guerrero-Mandujano A, Hernández-Cortez C, Ibarra JA, Castro-Escarpulli G. The outer membrane vesicles: secretion system type zero. Traffic. 2017;18(7):425–32.
8. Roier S, Zingl FG, Cakar F, Durakovic S, Kohl P, Eichmann TO, et al. A novel mechanism for the biogenesis of outer membrane vesicles in Gram-negative bacteria. Nat Commun. 2016;7:10515.
9. Skotland T, Llorente A, Sandvig K. Lipids in extracellular vesicles: what can be learned about membrane structure and function? Cold Spring Harb Perspect Biol. 2023;15(8): a041415.
10. van Niel G, D'Angelo G, Raposo G. Shedding light on the cell biology of extracellular vesicles. Nat Rev Mol Cell Biol. 2018;19(4):213–28.
11. Loeb MR, Kilner J. Release of a special fraction of the outer membrane from both growing and phage T4-infected *Escherichia coli* B. Biochim Biophys Acta. 1978;514(1):117–27.
12. Li M, Zhou H, Yang C, Wu Y, Zhou X, Liu H, et al. Bacterial outer membrane vesicles as a platform for biomedical applications: an update. J Control Release. 2020;323:253–68.
13. Holger DJ, Lev KL, Kebriaei R, Morrisette T, Shah R, Alexander J, et al. Bacteriophage-antibiotic combination therapy for multidrug-resistant *Pseudomonas aeruginosa*: in vitro synergy testing. J Appl Microbiol. 2022;133(3):1636–49.
14. Wayne P. CLSI. Performance standards for antimicrobial susceptibility testing. CLSI supplement M100. 32nd ed. Clinical and Laboratory Standards Institute; 2022.
15. Zhang X, Qian C, Tang M, Zeng W, Kong J, Fu C, et al. Carbapenemase-loaded outer membrane vesicles protect *Pseudomonas aeruginosa* by degrading imipenem and promoting mutation of antimicrobial resistance gene. Drug Resist Updat. 2023;68: 100952.
16. Hua Y, Wang J, Huang M, Huang Y, Zhang R, Bu F, et al. Outer membrane vesicles-transmitted virulence genes mediate the emergence of new antimicrobial-resistant hypervirulent *Klebsiella pneumoniae*. Emerg Microbes Infect. 2022;11(1):1281–92.
17. Shen HB, Chou KC. Gneg-mPLoc: a top-down strategy to enhance the quality of predicting subcellular localization of Gram-negative bacterial proteins. J Theor Biol. 2010;264(2):326–33.
18. Huang Y, Li J, Wang Q, Tang K, Cai X, Li C. Detection of carbapenem-resistant hypervirulent *Klebsiella pneumoniae* ST11-K64 co-producing NDM-1 and KPC-2 in a tertiary hospital in Wuhan. J Hosp Infect. 2023;131:70–80.
19. Lee J, Lee J, Cho Y, Choi J, Han SW. A putative 2,3-bisphosphoglycerate-dependent phosphoglycerate mutase is involved in the virulence, carbohydrate metabolism, biofilm formation, twitching halo, and osmotic tolerance in *Acidovorax citrulli*. Front Plant Sci. 2022;13:1039420.
20. Roth M, Goodall ECA, Pullela K, Jaquet V, François P, Henderson IR, et al. Transposon-directed insertion-site sequencing reveals glycolysis gene *gpmA* as part of the H(2)O(2) defense mechanisms in *Escherichia coli*. Antioxidants (Basel). 2022;11(10):2053.
21. Xia X, Liu J, Huang L, Zhang X, Deng Y, Li F, et al. Molecular details of actinomycin D-treated MRSA revealed via high-dimensional data. Mar Drugs. 2022;20(2):114.
22. Thoden JB, Firestine SM, Benkovic SJ, Holden HM. PurT-encoded glycinamide ribonucleotide transformylase. Accommodation of adenosine nucleotide analogs within the active site. J Biol Chem. 2002;277(26):23898–908.
23. Thoden JB, Firestine S, Nixon A, Benkovic SJ, Holden HM. Molecular structure of *Escherichia coli* PurT-encoded glycinamide ribonucleotide transformylase. Biochemistry. 2000;39(30):8791–802.

24. Gu Y, Huang L, Wu C, Huang J, Hao H, Yuan Z, et al. The evolution of fluoroquinolone resistance in *Salmonella* under exposure to sub-inhibitory concentration of enrofloxacin. Int J Mol Sci. 2021;22(22):12218.
25. Hayer-Hartl M, Bracher A, Hartl FU. The GroEL-GroES chaperonin machine: a nano-cage for protein folding. Trends Biochem Sci. 2016;41(1):62–76.
26. Goltermann L, Good L, Bentin T. Chaperonins fight aminoglycoside-induced protein misfolding and promote short-term tolerance in *Escherichia coli*. J Biol Chem. 2013;288(15):10483–9.
27. Goltermann L, Sarusie MV, Bentin T. Chaperonin GroEL/GroES overexpression promotes aminoglycoside resistance and reduces drug susceptibilities in *Escherichia coli* following exposure to sublethal aminoglycoside doses. Front Microbiol. 2015;6:1572.
28. Muri J, Kopf M. The thioredoxin system: balancing redox responses in immune cells and tumors. Eur J Immunol. 2023;53(1): e2249948.
29. May HC, Yu JJ, Guentzel MN, Chambers JP, Cap AP, Arulanandam BP. Repurposing auranofin, ebselen, and PX-12 as antimicrobial agents targeting the thioredoxin system. Front Microbiol. 2018;9:336.
30. AlOkda A, Van Raamsdonk JM. Evolutionarily conserved role of thioredoxin systems in determining longevity. Antioxidants (Basel). 2023;12(4):944.
31. Lee SJ, Tran NQ, Lee J, Richardson CC. Hydrophobic residue in *Escherichia coli* thioredoxin critical for the processivity of T7 DNA polymerase. Biochemistry. 2018;57(40):5807–17.

Publisher's Note